Journal of Cleaner Production 236 (2019) 117705

Contents lists available at ScienceDirect

Journal of Cleaner Production

journal homepage: www.elsevier.com/locate/jclepro

Water reuse nexus with resource recovery: On the fluidized-bed homogeneous crystallization of copper and phosphate from semiconductor wastewater

Lester Lee E. Bayon [a], Florencio C. Ballesteros Jr. [a], Sergi Garcia-Segura [b, *], Ming-Chun Lu [c, **]

[a] Environmental Engineering Graduate Program, College of Engineering, University of the Philippines, Diliman, Quezon City, Philippines
[b] Nanosystems Engineering Research Center for Nanotechnology-Enabled Water Treatment, School of Sustainable Engineering and the Built Environment, Arizona State University, Tempe, AZ, 85287-3005, United States
[c] Department of Environmental Resources Management, Chia Nan University of Pharmacy and Science, Tainan, Taiwan

ARTICLE INFO

Article history:
Received 24 March 2019
Received in revised form
21 June 2019
Accepted 17 July 2019
Available online 17 July 2019

Handling editor: Yutao Wang

Keywords:
Industrial wastewater treatment
Fluidized bed reactor
Resource recovery
Heavy metals
Waste revalorization

ABSTRACT

Green and sustainable strategies aim for the development of manufacturing processes that maximize the use of resources instigating semiconductor industry to adopt zero-liquid discharge policies. Complexity and variations of semiconductor wastewater effluents opens an opportunity for resource recovery (i.e. copper from chemical-mechanical polishing) including heavy metals and inorganic ions (i.e. phosphate from acid cleaning). This present work demonstrates the capabilities of fluidized-bed homogeneous crystallization as treatment technology to process water effluents for industrial reuse while simultaneously recovering precious resources such as copper and phosphate. Operational variables have been optimized considering the combination of both effluents to produce high quality copper phosphate granules. The optimum copper percentage removal and crystallization efficiency were 99% and 96.07% respectively obtained at pH_e 6.0–6.5, 1.25 $[PO_4^{-3}]_{in}/[Cu^{2+}]_{in}$ at hydraulic retention time 22.5 min with 0.51 kg Cu^{2+}/m^2 h and fixed $[Cu^{2+}]_{in}$ loading of 4.5 mM. The recovered crystals have an average particle diameter of ~1 mm and were characterized identifying libethenite (Cu_2PO_4OH) as main recovered products.

1. Introduction

Sustainable development should promote economic growth and technology development while simultaneously protecting the environment by implementing green production processes (Scarazzato et al., 2017; Zhang and Xu, 2018). Efficient environmental management strategies of complex industrial effluents are challenging and has been the primary objective of the scientific community. This prompted many researchers to design and develop technologies that can lead to zero liquid discharge and resource recovery from industrial effluent for further utilization (Cieślik and Konieczka, 2017). Semiconductor manufacturing involves various steps that generate specific effluent compositions generally combined in a sole wastewater effluent. Incorporation of cost-effective on-site treatment technologies in semiconductor industry is challenging due to the varied composition of each produced effluent (Akbal and Camcidotless, 2011; Speed et al., 2015). Combination of these singular waste streams results in a complex mixture wastewater that contains heavy metals, inorganic (Aoudj et al., 2017) and/or organics (Garcia-Segura and Brillas, 2017) species. Thus, identifying characteristic and composition of effluent composition at different specific steps is of great importance for the development of technologies for cleaner production.

In this scenario, fluidized-bed crystallization (FBC) technology emerges as alternative phase-separation technology designed to treat wastewater coming from semiconductor industry. The said engineered process relies in the same fundamental as conventional chemical precipitation, including the identification of insoluble species of ionic pollutants (e.g. heavy metals, inorganic ionic species) (Djedidi et al., 2008; Huang et al., 2017). However, the main

* Corresponding author.
** Corresponding author.
E-mail addresses: Sergio.Garcia.Segura@asu.edu (S. Garcia-Segura), mmclu@mail.cnu.edu.tw (M.-C. Lu).

https://doi.org/10.1016/j.jclepro.2019.117705
0959-6526/

difference is that FBC enhances crystal growth and allows the recovered solids for reuse (Lv et al., 2018; Su et al., 2014). Previous studies had demonstrated the resource recovery of valuable products such as struvite (Caddarao et al., 2018; Shih et al., 2017), iron salts (Mahasti et al., 2019; Priambodo et al., 2017), and lead carbonate (Chen et al., 2015; De Luna et al., 2015). Heterogeneous FBC utilizes seeds (e.g. silica sand) that initiate the precipitation of metal salts to form impure solid crystals (Aldaco et al., 2007; De Luna et al., 2017; Huang et al., 2007). Use of seeds of different chemical composition diminishes the purity of the product recovered that consequently decreases its economic value. In order to address this barrier, a novel fluidized-bed homogeneous crystallization (FBHC) has been designed to induce nucleation at a metastable region of low supersaturation that leads to the agglomeration of nuclei promoting homogeneous crystal growth (Ballesteros et al., 2016; Cheremisinoff and Davletshin, 2015; Shih et al., 2016). Thus, allowing high purity crystals formation and recovery for market exploitation (Westerhoff et al., 2015).

The present work identifies an opportunity for FBHC implementation on the management of semiconductor industry wastewater through the formation of highly insoluble copper phosphate granules. In chemical-mechanical polishing (CMP) process, the generated wastewater effluents are rich in heavy metals such as copper while acid cleaning and etching process produce effluents that contains high concentrations of phosphate. The simultaneous treatment of these two effluents can potentially lead to the removal of pollutants in wastewater while recovering phosphate and copper as re-valorizable products. As such, the main objective of the study is to identify the optimum operational conditions and effluent characteristics to attain high removals and homogeneous product recovery using the parameters of operating pH, concentration ratio of phosphate to copper, hydraulic retention time (HRT) and copper surface loading. The morphology of the recovered granules were determined by SEM and XRD analysis.

2. Experimental methods

2.1. Chemicals

Two synthetic wastewater effluents were prepared (i) using copper chloride dihydrate (>99% purity) and (ii) sodium hydrogen phosphate (>98% purity) both supplied by Choneye Pure Chemicals. Solution pH was adjusted with 1M solutions of nitric acid and/or sodium hydroxide purchased from BASF and Merck, respectively. Solutions were prepared with laboratory grade reverse osmosis water with resistivity >18.2 MΩ cm at 25 °C.

2.2. Fluidized-bed reactor system set-up

Scheme of Fig. 1 depicts the experimental set up using a fluidized-bed reactor (FBR) to treat 450 mL of solution. The reactor was composed of a cylindrical Pyrex glass column with two differentiated reactor zones: the inferior part of the reactor has an inner diameter of 2 cm and a height of 80 cm, while the superior part has a wider diameter of 4 cm within 20 cm height. The diameter expansion at the upper part of the reactor ensures successful granulation and recovery by preventing fines from draining out during recirculation. As depicted in Fig. 1, two feeding solution inlets (F1 and F2) are located at the inferior part delivering copper (II) and phosphate, respectively. Solution was continuously recirculated at constant flow rate using a peristaltic pump (Iwaki MD-10-NL2). Glass beads (5 mm) were set at the bottom of the fluidized-bed reactor to stimulate turbulence and ensure uniform flow distribution, and to prevent undesirable clogging of fines/granules.

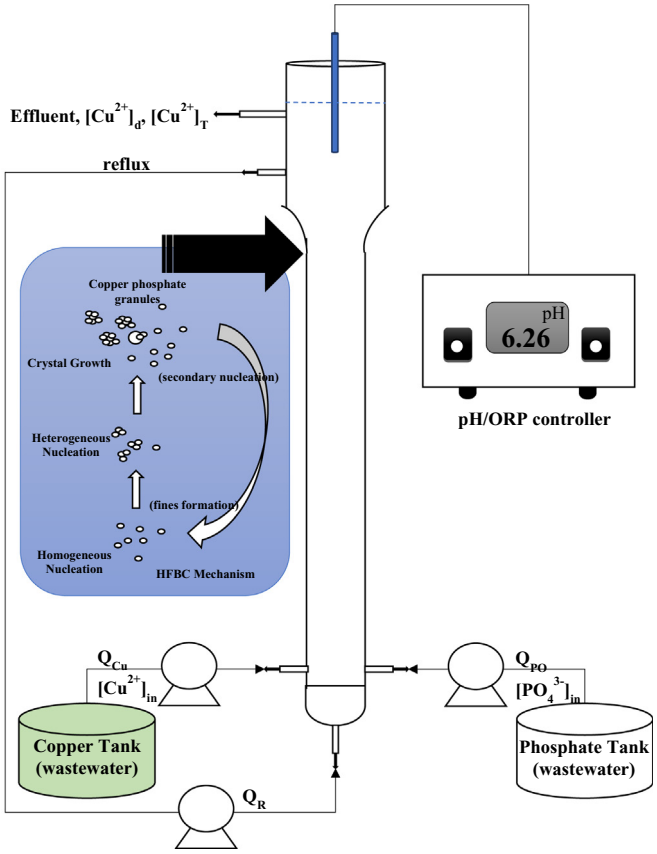

Fig. 1. Scheme of fluidized-bed reactor and granules formation mechanism.

2.3. Analytical procedures and instruments

Copper concentration was quantified from aqueous samples using an AAnlayst 200 Atomic Absorption Spectrometer (PerkinElmer). Total copper including fines ($[Cu^{2+}]_T$) was determined from unfiltered samples. Concentration of dissolved copper ions in effluent ($[Cu^{2+}]_d$) was determined from samples filtered with 0.45 μm membranes. Prior analysis filtered and non-filtered samples were digested with concentrated HNO_3 (APHA, 1999). Moreover, copper removal and granulation were calculated from these experimental results using equations (1) and (2):

$$\%\text{Removal} = \frac{[Cu]_0 - [Cu]_d}{[Cu]_0} \times 100 \quad (1)$$

$$\%\text{Granulation} = \frac{[Cu]_0 - [Cu]_T}{[Cu]_0} \times 100 \quad (2)$$

where $[Cu]_0$ is the initial concentration of copper to be treated in the reactor. Solution pH was continuously monitored by a pH/ORP controller PC-310 from Shin Shiang Tech Instruments. Solid copper phosphate granules formed during the FBHC treatment process were collected, air-dried and sieved for particle sized distribution analysis. To classify particle US sieve size numbers 18, 25, 50, and 40 were used. The granules were characterized by X-ray diffraction with a DX-2000 SSC diffractometer (Rigaku) by applying a Cu $K\alpha_{1+2}$ radiation ($\lambda(\alpha_1) = 0.154060$ nm and $\lambda(\alpha_2) = 0.154443$ nm) at 40 kV and 30 mA current.

3. Results and discussion

3.1. Understanding granulation recovery dependence with pH

Homogeneous crystallization in the FBHC process can be described as a continuous mass transfer of ions in aqueous phase to precipitate nuclei inducing crystal growth. FBHC requires the formation of initial nuclei, which is only attained when reaching certain degree of supersaturation. However, note that an excessive supersaturation state would result in the precipitation of fines but not crystal growth. Thus, crystallization in the fluidized state should be driven at low supersaturation to induce initial nucleation followed by crystal growth (Mahasti et al., 2017; Salcedo et al., 2016). Therefore, concentration of precipitant species and their speciation plays a significant role in FBHC process. The following description provides a framework of understanding of the species involved in the resource recovery process of effluents containing phosphate and copper.

Phosphoric acid is a triprotic acid widely used during semiconductors manufacturing processes for acid cleaning and etching (Warmadewanthi and Liu, 2009). Effluents containing phosphate species results from this manufacturing step. The low solubility of certain metallic phosphates encourages the possible combination of these industrial effluents for strategic resource recovery. Moreover, phosphate ions speciation distribution is tightly related to effluent pH according to the acid-base equilibria described by reactions (3)–(5) (Caddarao et al., 2018).

$$H_3PO_4 \leftrightharpoons H^+ + H_2PO_4^- \quad pK_{a1} = 2.15 \tag{3}$$

$$H_2PO_4^- \leftrightharpoons H^+ + HPO_4^{2-} \quad pK_{a2} = 7.20 \tag{4}$$

$$HPO_4^{2-} \leftrightharpoons H^+ + PO_4^{3-} \quad pK_{a3} = 12.35 \tag{5}$$

Different insoluble copper species and their corresponding solubility product (K_{sp}) as reported in literature are shown in Table 1. The said species can be formed in the presence of phosphate ions at different pH range. Fig. 2 shows the solubility diagram of the stability regions of different species as a function of pH. The diagram suggests a preferential region of libethenite (Cu_2PO_4OH) precipitation in a pH range of 4.5–8.5.

Identifying the optimum pH condition is necessary to ensure maximum removal of copper and phosphate through precipitation of insoluble species from the selective combination of the said two wastewater effluents from semiconductor industry. Operational pH also plays a significant role in the supersaturation conditions management impacting on granule recovery capabilities of FBHC process. Fig. 3 illustrates the copper removal percentage obtained from the FBHC treatment of copper and phosphate effluents at the concentration of 4.5 mM (300 mg L^{-1}) and 5.6 mM (528 mg L^{-1}), respectively.

Copper ions are completely removed by precipitation when operating pH reaches 6.0. The profile of $[Cu^{2+}]_T$ depicts a dramatic decrease in concentration from 70 mg L^{-1} (pH 4.5) down to 10 mg L^{-1} (pH 6.0–6.5). However $[Cu^{2+}]_T$ increases dramatically

Table 1
Solubility product constants (K_{sp}) of different copper salt species.

Copper salts	K_{sp}	References
Copper Phosphate, $Cu_3(PO_4)_2$	−36.85	Aksu (2009)
Libethenite, Cu_2PO_4OH	−28.00	Selim (2015)
Copper hydroxide, $Cu(OH)_2$	−14.70	Zhou et al. (1999)
Copper carbonate, $CuCO_3$	−9.85	Lee et al. (2004)

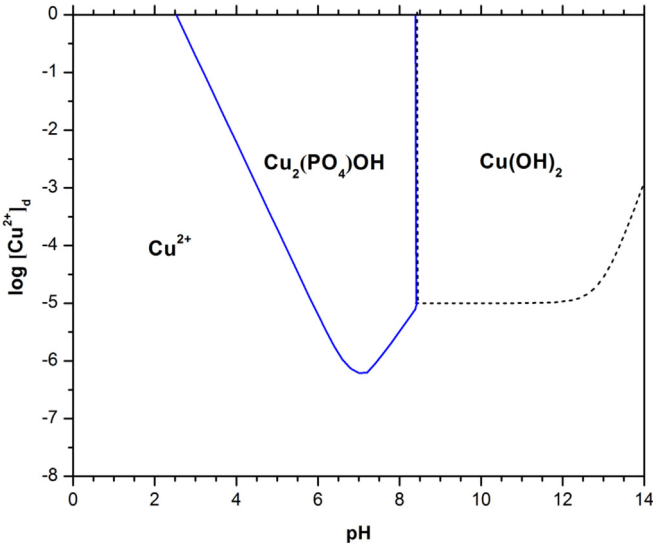

Fig. 2. Solubility diagram of copper in presence of phosphate (assumed $[PO_4^{3-}]_0 = 10^{-2}$ M).

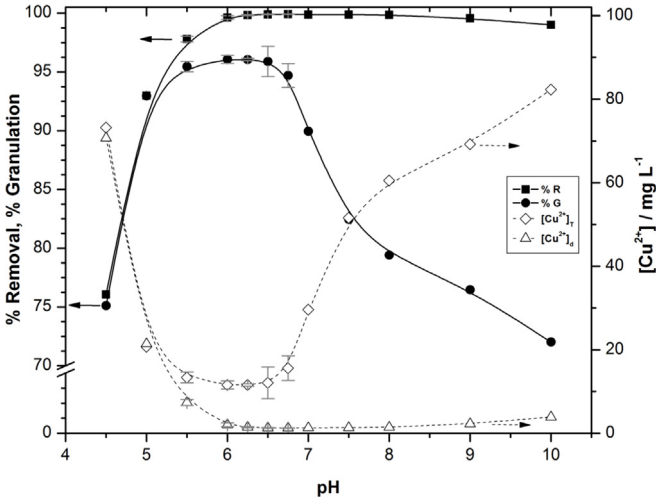

Fig. 3. Effects of pH on (■) copper removal and (●) copper phosphate granulation during the FBHC treatment of $[Cu^{2+}]_0 = 4.5$ mM (~300 mg L^{-1}) at $[PO_4^{3-}]/[Cu^{2+}] = 1.25$ ratio with HRT = 22.5 min, U = 28.65 m h^{-1}, $Q_{Cu} = Q_{PO4} = 10$ mL min^{-1}). Profiles of (◇) $[Cu^{2+}]_d$ and (Δ) $[Cu^{2+}]_T$ are depicted for each pH operational condition evaluated.

with increasing pH values above 6.5 which allows inferring a preferential nucleation mechanism over crystal growth. This agrees with the yield of higher amount of fines no recoverable that must be removed from the FBHC effluent by conventional filtration (Kozik et al., 2014). Thus, Fig. 3 allows clearly identifying close to circumneutral pH 6.0–6.5 as the optimum operational conditions with a granulation recovery of 96.0%. Note that these mild of conditions are highly beneficial for a treatment train since treated effluents would not require pH neutralization post-treatment prior water reuse or release.

The particle size distribution of the recovered granules which depends on operational pH provides an insight on the applicability of FBHC on the recovery of copper and phosphate from semiconductor manufacturing. The spheroidal shaped granules were obtained due to the fluidization of the solids that precipitated within the fluidized-bed reactor (Binev et al., 2015). Fig. 4 illustrates

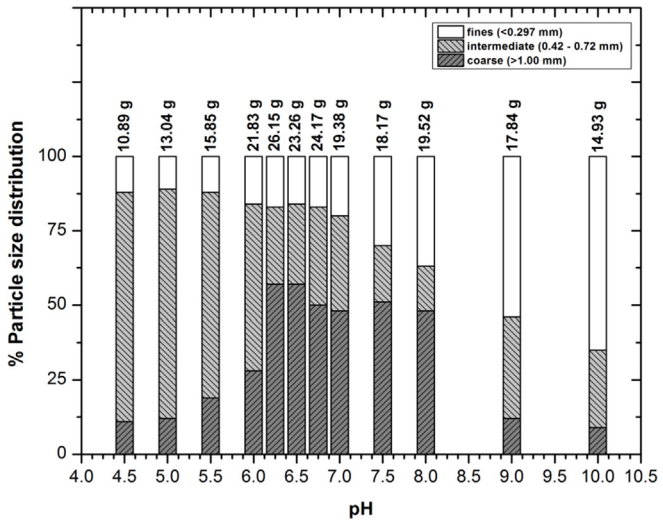

Fig. 4. Particle size distribution of recovered granules after FBHC treatment under different operational pH to induce crystallization.

the influence of pH on the recovery capabilities of FBHC and on the size distribution of granules obtained. Note that over 20 g were recovered at pH range of 6.0–7.0. The maximum solid mass collected under pH 6.25 was (26.15 g), 55% of which were characterized as coarse granules (>1.00 mm in diameter). Theoretical calculation based on the total copper fed during the system indicates that maximum solid libethenite ($Cu_2(PO_4)OH$) recoverable is 32.25 g, therefore attaining a maximum recovery of 81% at pH 6.25. Variation on the size distribution were observed at different pH range, which demonstrate the preferential crystal growth of coarse granules over 1.00 mm of diameter. Meanwhile values as low as 10% coarse were recovered at acidic and extremely alkaline conditions of pH 4.5 and 10.0, respectively. It can be observed that 65% fine particles with diameter size smaller than 0.297 mm were collected at pH 10.0, as displayed in the results of Fig. 3. Supersaturation condition at pH 10.0 promotes the formation of small nuclei that are not easily recovered and may be washed out from the reactor. On top of that, these experimental conditions do not favor crystal growth which results then in the formation of smaller granules as demonstrated by the size distribution analyses. In this frame, these results suggest that nucleation is promoted over crystal growth at alkaline pH which may difficult the recovery of reusable solids. Likewise, higher pH conditions may promote the co-precipitation of other insoluble copper species (i.e. $Cu(OH)_2$) different than phosphate (as shown in Fig. 2) which not only decreases phosphate removal but also diminishes the purity of the recovered product and the FBHC selectivity towards preferential precipitates (Guillard and Lewis, 2001).

3.2. Concentration ratio of the fed wastewater effluents effects on the FBHC performance

Insoluble crystals of Cu_2PO_4OH are formed inside the FBHC reactor during the mixture of two synthetic industrial effluents resulting to: (i) copper-rich CMP wastewater and (ii) phosphate-rich acid cleaning wastewater. The $[PO_4^{3-}]/[Cu^{2+}]$ ratio dictates supersaturation condition and therefore affects the physical phase separation (by precipitation) and crystal recovery capabilities of FBHC process. Fig. 5 demonstrates the granulation recovery of copper-rich CMP effluents (4.5 mM) at increasing phosphate concentration from the $[PO_4^{3-}]/[Cu^{2+}]$ ratio of 0.5–4.0. The maximum granulation recovery (96%) was obtained at optimum zone between 1.0 and 1.5 ratio while the stoichiometric concentrations at 0.5 ratio revealed incomplete pollutant removal and significant decrease on the granulation recovery (ca. 77%). It can be deduced from Fig. 5 that excessive concentration of phosphate is not favorable as it decreases the granules recovery to as low as 75%. This trend can be explained by the high supersaturation induced under high

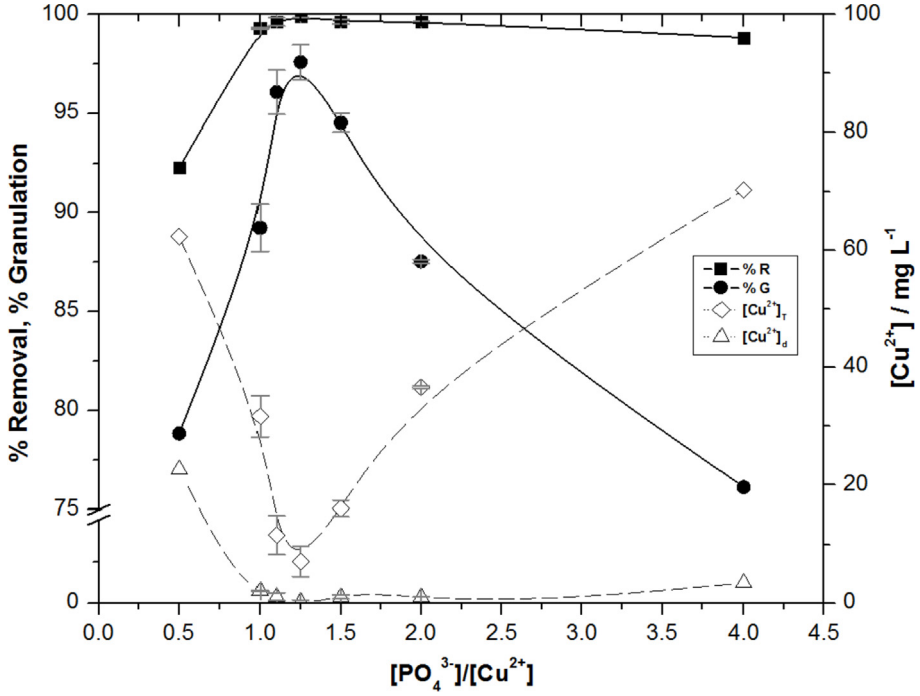

Fig. 5. Influence of $[PO_4^{3-}]/[Cu^{2+}]$ ratio on the FBHC treatment performance when treating an effluent of $[Cu^{2+}]_0 = 4.5$ mM (~300 mg L^{-1}) at pH = 6.25 ± 0.1 (HRT = 22.5 min, U = 28.65 m h^{-1}, $Q_{Cu} = Q_{PO4} = 10$ mL min^{-1}). Profiles of (■) percentage of removal, (●) percentage of granulation, (◇) $[Cu^{2+}]_d$ and (Δ) $[Cu^{2+}]_T$ are depicted for each operational molar ratio.

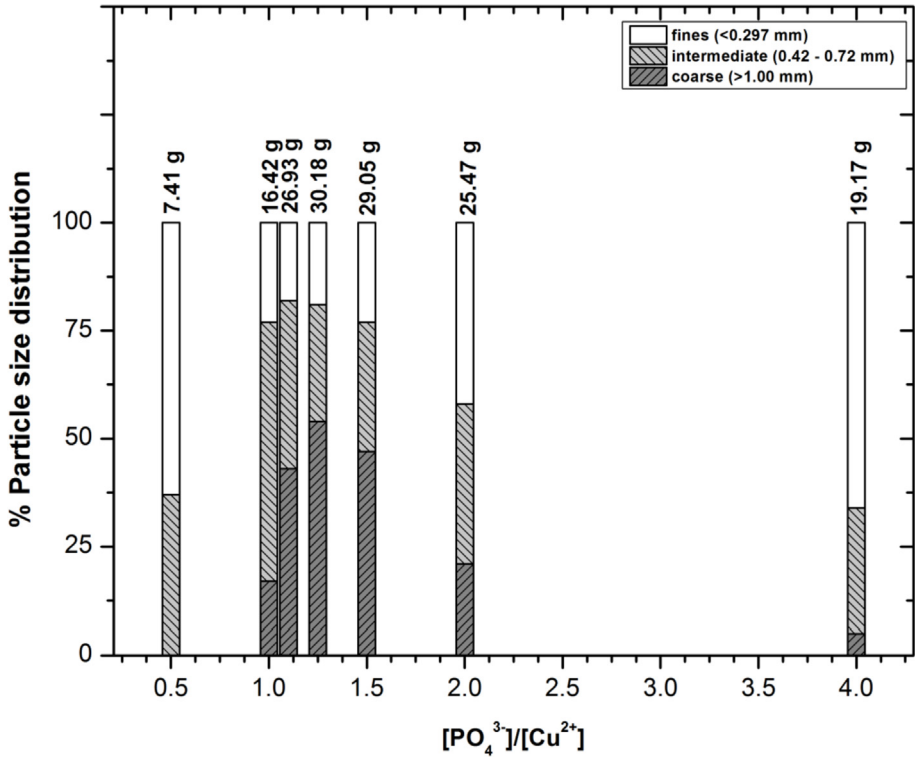

Fig. 6. Operational $[PO_4^{3-}]/[Cu^{2+}]$ ratio effect on recovered granule size distribution.

concentration of phosphate that results to the preferential condition of the nucleation of fines causing more suspended solids on effluent that will be discharged to treated bodies of water (Pahunang et al., 2018).

For industrial wastewater effluent standards, the total suspended solids should be ≤ 30 mg L^{-1} specifically for semiconductor manufacturing as prescribed by environmental protection agencies (US EPA, 2016). The treated effluents above ratio of 2.0 (see Fig. 5) surpass the standard TSS values which is not recommended as it requires additional filtration process (Hamoda et al., 2004). Also, it was observed that the increase of total copper concentration is directly proportional to the increasing concentration of phosphate-rich in the acid cleaning effluent. Conversely, optimization of $[PO_4^{3-}]/[Cu^{2+}]$ ratio can minimize suspended solids and enhance granules recovery with maximum copper removal from industrial effluents. The results on the effects of the $[PO_4^{3-}]/[Cu^{2+}]$ molar ratio over 2.0 are in good agreement with the deceleration of crystal growth kinetics over nucleation at high supersaturation conditions (Bhuiyan et al., 2008).

The influence of $[PO_4^{3-}]/[Cu^{2+}]$ molar ratio on the crystal size distribution was described on Fig. 6. Maximum crystal growth occurs at the range of molar ratio 1.0–2.0. At this condition, coarse granules with size larger than 1 mm of diameter (>40%) were obtained. The results exhibit the direct impact of fed ratio concentration of phosphate-rich and copper-rich wastewater effluents on FBHC performance in terms of resource recovery capabilities and crystal quality control. Moreover, the optimum condition for maximum pollutants removal and higher granulation recovery was achieved at $[PO_4^{3-}]/[Cu^{2+}]$ molar ratio of 1.25.

3.3. Controlling effluents fed maximizes recovery: on the effect of loading per cross-section area

Experimental results demonstrate the excellent removal of copper and phosphate ions thru precipitation was attained at pH value starting from 6.0 and above as supported by the solubility diagram (Fig. 2). Likewise, almost complete removal was realized when fed molar ratio $[PO_4^{3-}]/[Cu^{2+}]$ is above 1.0. However, the influence of operational variables should be observed in terms of its granulation capability. This is related to the efficient control of the supersaturation conditions to induce not only the initial nucleation to form homogeneous seeds, but mostly to warrant crystal growth for granule recovery (Chen et al., 2015; Mahasti et al., 2017).

It is important to remark that nucleation and growth occurs in

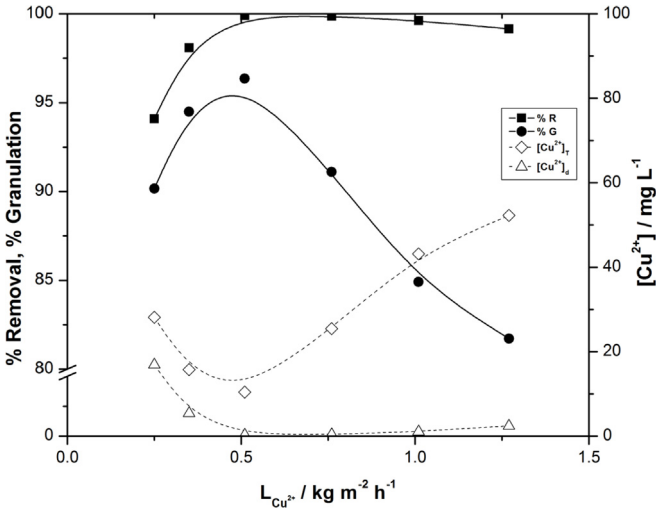

Fig. 7. Influence of copper surface loading (L_{Cu}) during FBHC treatment of $[Cu^{2+}]_0 = 4.5$ mM (~300 mg L^{-1}) with $[PO_4^{3-}]/[Cu^{2+}]$ ratio 1.25 at pH = 6.25 ± 0.1. Profiles of (■) percentage of removal, (●) percentage of granulation, (◇) $[Cu^{2+}]_d$ and (Δ) $[Cu^{2+}]_T$ are depicted for each L_{Cu}.

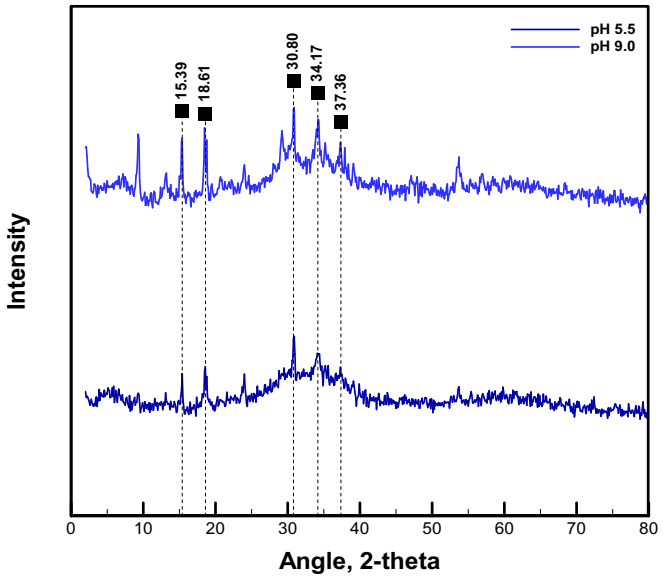

Fig. 8. X-ray diffractograms of granules with characteristic Libethenite ($Cu_2(PO_4)OH$) peaks.

region of sudden expansion inside the FBR (see Fig. 1). Supersaturation conditions are defined by the hydrodynamic parameters that control the surface loading (L), that denotes the rate of flow of pollutant species through the cross-sectional area of the lower column of FBR according to equation below:

$$L = \frac{Q_P\,[P]_{in}}{A_1} \tag{6}$$

where Q_P is the influx flow rate (L h^{-1}) of polluted wastewater effluent (copper or phosphate), $[P]_{in}$ the initial concentration of pollutant in the influent reservoir (kg L^{-1}), and A_1 is the cross sectional area of lower column ($3.14 \times 10^{-4}\,m^2$ for the reactor used).

FBHC was evaluated in terms of L_{Cu} under optimized conditions of operational pH and molar ratio $[PO_4^{3-}]/[Cu^{2+}]$. Moreover, optimized L_{Cu} was determined by varying the total influx flow rates (Q_T) which is the sum of the fed wastewater effluents of copper and phosphate ($Q_{PO4} = Q_{Cu}$). Fig. 7 depicts the effect of L_{Cu} on removal and granulation of libethenite by FBHC. It can be deduced that low L_{Cu} dilutes the concentration of precipitants in the fluidized chamber resulting in a lower supersaturation condition that do not allow complete abatement of copper concentration in treated effluent. Also, there is a noticeable increase in concentration of suspended fine nuclei at increasing L_{Cu}. The said increase can be explained by the attainment of high supersaturation conditions in the continuous flow reactor that favor nucleation of the fines over crystal growth while decreasing the recovery of Cu_2PO_4OH.

There is a clear identification of the region where minimum suspended solids occurs, which suggest optimum supersaturation conditions that induce crystal growth for granule recovery $[Cu]_T$. The determined optimum L_{Cu} region is about 0.5 kg m^{-2} h^{-1} (equivalent to $Q_{Cu} = Q_{PO} = 10$ mL min^{-1}). The overall outcomes suggest that excellent pollutant removal is dependent on the L_{Cu} and L_{PO4} and not on the initial concentration of feed wastewater effluent. The accurate control of L_{Cu} and L_{PO4} results to adequate $[PO_4^{3-}]/[Cu^{2+}]$ molar ratio of 1.25 that influence high degrees of pollutant removal for water reuse and resource recovery.

3.4. Crystals characterization of Cu_2PO_4OH granules

The recovered copper phosphates granules were characterized under the following optimal conditions: $[Cu^{2+}]_{in}$ 4.50 mM (~285 mg L^{-1}), pH_e 6.25 ± 0.1 and $[PO_4^{3-}]/[Cu^{2+}]$ of 1.25 with a constant hydraulic parameter of $Q_{Cu} = Q_P = 10$ mg L^{-1} and HRT 22.50 min. Diffractographic analysis by XRD identifies the presence of copper phosphate hydroxide $Cu_2(PO_4)OH$ crystals with libethenite mineral as main component. The said libethenite having orthorhombic crystal phase as characteristized through its diffraction peaks at 2θ values of 15.39, 18.61, 30.80, 34.17, 37.36 and 15.39, 18.57, 30.76, 3.31, 37.21 as shown in Fig. 8. Characterization results agree with the species identified in the solubility diagram of Fig. 2 for equilibrium conditions.

Macroscopic image in Fig. 9 shows that the morphologies of turquoise copper granules formed smooth surfaces. Granules recovered were further analyzed by SEM showing a uniform structure with a fluidized spheroidal structure, which suggest uniform crystal growth in fluidized state.

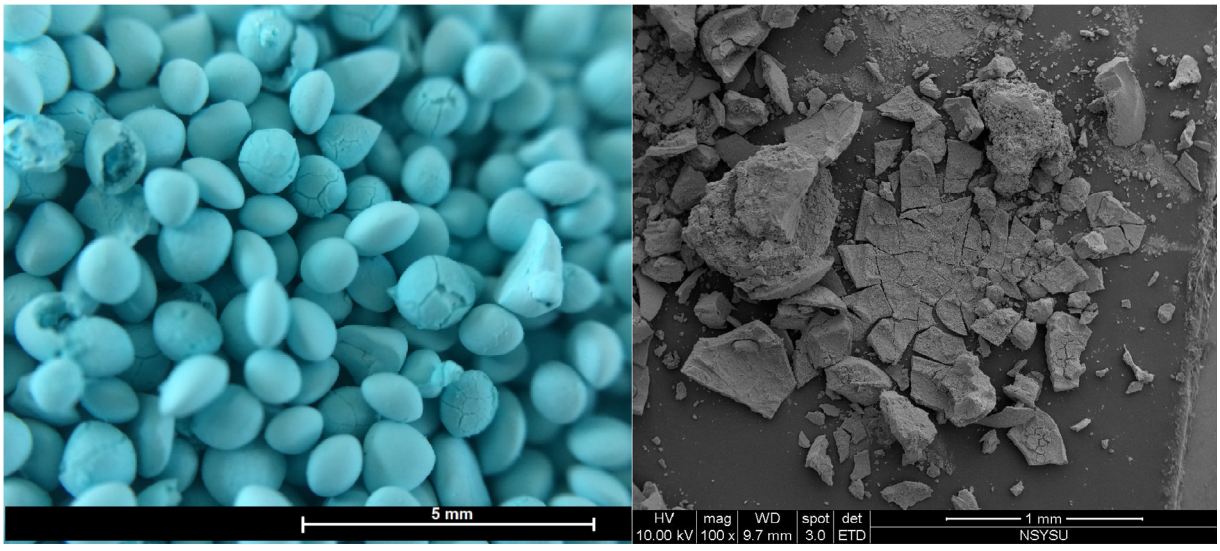

Fig. 9. Macroscopic and SEM images of Libethenite granules.

4. Conclusion

Strategic use of wastewater effluents of different manufacturing stages of semiconductor industry appears as alternative cleaner production management approach. Combination of copper containing effluents from chemical-mechanical and acid cleaning effluents containing high loads of phosphate anion can be used as fed water for fluidized-homogeneous crystallization for resource recovery and water treatment. As such, fluidized-bed homogeneous crystallization emerges as alternative treatment for zero-liquid discharge strategies allowing resources recovery from semiconductor wastewater industry.

The overall results shows the influence of pH on the heavy metal recovery and crystallization growth. The said observation was demonstrated on the solubility diagram of copper insoluble species and the marked speciation of phosphate anions with pH. It was observed that resource recovery and pollutant removal from water can be attained at mild condition of treatment of pH 6.0–6.5, which is desired for treated effluent discharge or reuse. Moreover, $[PO_4^{3-}]/[Cu^{2+}]$ molar ratio shows the influence on recovered granule sizes and copper concentration decay. An optimum ratio of 1.25 when treating conventional concentrations of copper at 285 mg L^{-1} (4.5 mM) shows a complete copper removal and 96% granulation recovery was obtained under these optimum conditions with hydraulic retention times of 22.5 min and surface loadings of 0.51 kg Cu^{2+}/m^2h. The granules recovered were characterized to have selective crystallization of libethenite as main product.

Acknowledgements

The authors would like to thank the Ministry of Science and Technology, Taiwan (MOST 107-2221-E-041-001-MY3) and the Department of Science and Technology, Philippines for funding of this research.

References

Akbal, F., Camcidotless, S., 2011. Copper, chromium and nickel removal from metal plating wastewater by electrocoagulation. Desalination 269, 214–222. https://doi.org/10.1016/j.desal.2010.11.001.

Aksu, S., 2009. Electrochemical equilibria of copper in aqueous phosphoric acid solutions. J. Electrochem. Soc. 156, C387–C394. https://doi.org/10.1149/1.3215996.

Aldaco, R., Garea, A., Irabien, A., 2007. Calcium fluoride recovery from fluoride wastewater in a fluidized bed reactor. Water Res. 41, 810–818. https://doi.org/10.1016/j.watres.2006.11.040.

Aoudj, S., Khelifa, A., Drouiche, N., 2017. Removal of fluoride, SDS, ammonia and turbidity from semiconductor wastewater by combined electrocoagulation–electroflotation. Chemosphere 180, 379–387. https://doi.org/10.1016/j.chemosphere.2017.04.045.

APHA, 1999. Standard methods for examination of water and wastewater., American public health association, American water works association and water environmental federation: Washington, DC, USA https://doi.org/ISBN 9780875532356.

Ballesteros, F.C., Salcedo, A.F.S., Vilando, A.C., Huang, Y.H., Lu, M.C., 2016. Removal of nickel by homogeneous granulation in a fluidized-bed reactor. Chemosphere 164, 59–67. https://doi.org/10.1016/j.chemosphere.2016.08.081.

Bhuiyan, M.I.H., Mavinic, D.S., Beckie, R.D., 2008. Nucleation and growth kinetics of struvite in a fluidized bed reactor. J. Cryst. Growth 310, 1187–1194. https://doi.org/10.1016/j.jcrysgro.2007.12.054.

Binev, D., Seidel-Morgenstern, A., Lorenz, H., 2015. Study of crystal size distributions in a fluidized bed crystallizer. Chem. Eng. Sci. 133, 116–124. https://doi.org/10.1016/j.ces.2014.12.041.

Caddarao, P.S., Garcia-Segura, S., Ballesteros, F.C., Huang, Y.H., Lu, M.C., 2018. Phosphorous recovery by means of fluidized bed homogeneous crystallization of calcium phosphate. Influence of operational variables and electrolytes on brushite homogeneous crystallization. J. Taiwan Inst. Chem. Eng. 83, 124–132. https://doi.org/10.1016/j.jtice.2017.12.009.

Chen, C.S., Shih, Y.J., Huang, Y.H., 2015. Remediation of lead (Pb(II)) wastewater through recovery of lead carbonate in a fluidized-bed homogeneous crystallization (FBHC) system. Chem. Eng. J. 279, 120–128. https://doi.org/10.1016/j.cej.2015.05.013.

Cheremisinoff, N.P., Davletshin, A., 2015. Hydraulic Fracturing Operations: Handbook of Environmental Management Practices. John Wiley & Sons, Inc., Hoboken, New Jersey and Scrivener Publishing LLC, Salem, Massachusetts. https://doi.org/10.1002/9781119099987.

Cieślik, B., Konieczka, P., 2017. A review of phosphorus recovery methods at various steps of wastewater treatment and sewage sludge management. The concept of "no solid waste generation" and analytical methods. J. Clean. Prod. 142, 1728–1740. https://doi.org/10.1016/j.jclepro.2016.11.116.

De Luna, M.D.G., Bellotindos, L.M., Asiao, R.N., Lu, M.C., 2015. Removal and recovery of lead in a fluidized-bed reactor by crystallization process. Hydrometallurgy 155, 6–12. https://doi.org/10.1016/j.hydromet.2015.03.009.

De Luna, M.D.G., Rance, D.P.M., Bellotindos, L.M., Lu, M.C., 2017. Removal of sulfate by fluidized bed crystallization process. J. Environ. Chem. Eng. 5, 2431–2439. https://doi.org/10.1016/j.jece.2017.04.052.

Djedidi, Z., Tyagi, R.D., Cheikh, R. Ben, Blais, J.F., Mercier, G., 2008. Metals precipitation from effluents: review. Pract. Period. Hazard. Toxic, Radioact. Waste Manag. 12, 135–149 (2008)12:3(135). https://doi.org/10.1061/(asce)1090-025x.

Garcia-Segura, S., Brillas, E., 2017. Applied photoelectrocatalysis on the degradation of organic pollutants in wastewaters. J. Photochem. Photobiol. C Photochem. Rev. 31, 1–35. https://doi.org/10.1016/j.jphotochemrev.2017.01.005.

Guillard, D., Lewis, A.E., 2001. Nickel carbonate precipitation in a fluidized-bed reactor. Ind. Eng. Chem. Res. 40, 5564–5569. https://doi.org/10.1021/ie010312q.

Hamoda, M.F., Al-Ghusain, I., AL-Mutairi, N.Z., 2004. Sand filtration of wastewater for tertiary treatment and water reuse. Desalination 164, 203–211. https://doi.org/10.1016/S0011-9164(04)00189-4.

Huang, C., Pan, J.R., Lee, M., Yen, S., 2007. Treatment of high-level arsenic-containing wastewater by fluidized bed crystallization process. J. Chem. Technol. Biotechnol. 82, 289–294. https://doi.org/10.1002/jctb.1671.

Huang, H., Liu, J., Zhang, P., Zhang, D., Gao, F., 2017. Investigation on the simultaneous removal of fluoride, ammonia nitrogen and phosphate from semiconductor wastewater using chemical precipitation. Chem. Eng. J. 307, 696–706. https://doi.org/10.1016/j.cej.2016.08.134.

Kozik, A., Hutnik, N., Piotrowski, K., Matynia, A., 2014. Continuous reaction crystallization of struvite from diluted aqueous solution of phosphate(V) ions in the presence of magnesium ions excess. Chem. Eng. Res. Des. 92, 481–490. https://doi.org/10.1016/j.cherd.2013.08.032.

Lee, C.I., Yang, W.F., Hsieh, C.I., 2004. Removal of Cu(II) from aqueous solution in a fluidized-bed reactor. Chemosphere 57, 1173–1180. https://doi.org/10.1016/j.chemosphere.2004.08.028.

Lv, X. mei, Li, J., Chen, H., Tang, H. jiang, 2018. Copper wastewater treatment with high concentration in a two-stage crystallization-based combined process. Environ. Technol. 39, 2346–2352. https://doi.org/10.1080/09593330.2017.1354925.

Mahasti, N.N.N., Shih, Y.J., Huang, Y.H., 2019. Removal of iron as oxyhydroxide (FeOOH) from aqueous solution by fluidized-bed homogeneous crystallization. J. Taiwan Inst. Chem. Eng. 96, 496–502. https://doi.org/10.1016/j.jtice.2018.12.022.

Mahasti, N.N.N., Shih, Y.J., Vu, X.T., Huang, Y.H., 2017. Removal of calcium hardness from solution by fluidized-bed homogeneous crystallization (FBHC) process. J. Taiwan Inst. Chem. Eng. 78, 378–385. https://doi.org/10.1016/j.jtice.2017.06.040.

Pahunang, R.R., Lu, M.-C., Vilando, A.C., Ballesteros, F.C., de Luna, M.D.G., 2018. Optimum recovery of phosphate from simulated wastewater by unseeded fluidized-bed crystallization process. Separ. Purif. Technol. 212, 783–790. https://doi.org/10.1016/j.seppur.2018.11.087.

Priambodo, R., Tan, Y.L., Shih, Y.J., Huang, Y.H., 2017. Fluidized-bed crystallization of iron phosphate from solution containing phosphorus. J. Taiwan Inst. Chem. Eng. 80, 247–254. https://doi.org/10.1016/j.jtice.2017.07.004.

Salcedo, A.F.M., Ballesteros, F.C., Vilando, A.C., Lu, M.C., 2016. Nickel recovery from synthetic Watts bath electroplating wastewater by homogeneous fluidized bed granulation process. Separ. Purif. Technol. 169, 128–136. https://doi.org/10.1016/j.seppur.2016.06.010.

Scarazzato, T., Panossian, Z., Tenório, J.A.S., Pérez-Herranz, V., Espinosa, D.C.R., 2017. A review of cleaner production in electroplating industries using electrodialysis. J. Clean. Prod. 168, 1590–1602. https://doi.org/10.1016/j.jclepro.2017.03.152.

Selim, H., 2015. Phosphate in Soils: Interaction with Micronutrients, Radionuclides and Heavy Metals. CRC Press Taylor & Francis Group, Boca Raton, Florida. https://doi.org/10.2136/sssaj2015.0005br.

Shih, Y.J., Abarca, R.R.M., de Luna, M.D.G., Huang, Y.H., Lu, M.C., 2017. Recovery of phosphorus from synthetic wastewaters by struvite crystallization in a fluidized-bed reactor: effects of pH, phosphate concentration and coexisting ions. Chemosphere 173, 466–473. https://doi.org/10.1016/j.chemosphere.2017.01.088.

Shih, Y.J., Chang, H.C., Huang, Y.H., 2016. Reclamation of phosphorus from aqueous solutions as alkaline earth metal phosphate in a fluidized-bed homogeneous crystallization (FBHC) process. J. Taiwan Inst. Chem. Eng. 62, 177–186. https://doi.org/10.1016/j.jtice.2016.02.002.

Speed, D., Westerhoff, P., Sierra-Alvarez, R., Draper, R., Pantano, P., Aravamudhan, S., Chen, K.L., Hristovski, K., Herckes, P., Bi, X., Yang, Y., Zeng, C., Otero-Gonzalez, L., Mikoryak, C., Wilson, B.A., Kosaraju, K., Tarannum, M., Crawford, S., Yi, P., Liu, X., Babu, S.V., Moinpour, M., Ranville, J., Montano, M., Corredor, C., Posner, J., Shadman, F., 2015. Physical, chemical, and in vitro toxicological characterization of nanoparticles in chemical mechanical planarization suspensions used in the semiconductor industry: towards environmental health and safety assessments. Environ. Sci. Nano 2, 227–244. https://doi.org/10.1039/c5en00046g.

Su, C.C., Reano, R.L., Dalida, M.L.P., Lu, M.C., 2014. Barium recovery by crystallization

in a fluidized-bed reactor: effects of pH, Ba/P molar ratio and seed. Chemosphere 105, 100–105. https://doi.org/10.1016/j.chemosphere.2014.01.005.
US EPA, O., 2016. Effluent guidelines. Environ. Prot. Agency 15–19.
Warmadewanthi, Liu, J.C., 2009. Recovery of phosphate and ammonium as struvite from semiconductor wastewater. Separ. Purif. Technol. 64, 368–373. https://doi.org/10.1016/j.seppur.2008.10.040.
Westerhoff, P., Lee, S., Yang, Y., Gordon, G.W., Hristovski, K., Halden, R.U., Herckes, P., 2015. Characterization, recovery opportunities, and valuation of metals in municipal sludges from U.S. Wastewater treatment plants nationwide. Environ. Sci. Technol. 49, 9479–9488. https://doi.org/10.1021/es505329q.
Zhang, L., Xu, Z., 2018. A critical review of material flow, recycling technologies, challenges and future strategy for scattered metals from minerals to wastes. J. Clean. Prod. 202, 1001–1025. https://doi.org/10.1016/j.jclepro.2018.08.073.
Zhou, P., Huang, J.C., Li, A.W.F., Wei, S., 1999. Heavy metal removal from wastewater in fluidized bed reactor. Water Res. 33, 1918–1924. https://doi.org/10.1016/S0043-1354(98)00376-5.